Band structure, cohesive energy, optical conductivity, and Compton profile of lithium*

W. Y. Ching and J. Callaway
Department of Physics and Astronomy, Louisiana State University, Baton Rouge, Louisiana 70803
(Received 4 March 1974)

A self-consistent calculation of energy bands in lithium has been performed using the linear-combination-of-atomic-orbitals (LCAO) method. The basis set consisted of nine s-type, six p-type, and three d-type Gaussian orbitals. Exchange was included according to the $X\alpha$ method with $\alpha=2/3$. Results are presented for the band structure, Fermi-surface properties, cohesive energy, and the Compton profile. The interband contribution to the optical conductivity was calculated including the $\vec{k}$ variation of the momentum matrix elements. The distortions of the Fermi surface from spherical symmetry are less than 4%. The optical and thermal effective-mass ratios are 1.48 and 1.53, respectively. The onset of direct interband transitions is predicted to occur at 3.28 eV. The calculated cohesive energy is 0.124 Ry.

I. INTRODUCTION

The band structure of lithium has been studied by many authors.[1–21] We have undertaken another calculation with the following objectives: (i) to develop and test procedures for calculating energy bands within the linear-combination-of-atomic-orbitals (LCAO) method using as basis states individual Gaussian orbitals (not atomic functions); (ii) to calculate the total energy as a test of the numerical precision of our calculational methods; and (iii) to test the ability of ordinary band theory to predict the observed Compton profile and interband optical conductivity.

The LCAO or tight-binding method, as originally developed, was based on an expansion of the wave function for a band electron in a set of trial Bloch functions formed from wave functions for isolated atoms. The method was plagued by severe problems involving the computation of the numerous required integrals, particularly three-center integrals. The calculational difficulties were greatly reduced by Lin and collaborators,[14,17] who showed that the use of a Fourier expansion for the crystal potential eliminated the necessity for explicit consideration of three-center integrals, and pointed out the utility of Gaussian-type orbitals (GTO) as basis functions for the expansion. In previous work, the band structures of transition metals have been investigated using a basis set consisting of atomic wave functions (expressed as linear combinations of GTO) for all states except $3d$, and independent GTO for the $3d$.[22] The variational freedom of the basis sets would be increased and the accuracy of the results improved, if it were possible to treat the orbitals as independent. The present work is our first calculation of this type.

This calculation begins with the assumption of a charge density formed by the superposition of atomic charge densities, as determined from the work of Huzinaga.[23] Exchange was included according to the $X\alpha$ method,[24] with $\alpha=\frac{2}{3}$. Self-consistency was achieved by iteration, as described elsewhere.[25] In order to test the numerical accuracy achieved in this calculation, we have computed the total energy per atom. Comparison with the corresponding figure for an isolated lithium atom leads to a value for the cohesive energy of the metal. We have also used the calculated wave functions to compute the Compton profile, which is a measure of the electron momentum distribution.

Major emphasis in this work has been placed on calculation of the optical conductivity. In previous work, we have demonstrated that the interband contribution to the optical conductivity of potassium[26] can be adequately calculated using the self-consistent LCAO method. However, that work used a basis set consisting of atomic wave functions. The use of an individual orbital basis should lead to a substantial improvement in the wave functions of excited states. As a result, the conductivity calculated here should be accurate within the limitations of the one-electron approximation and the form of the exchange interaction employed. Of course, additional contributions must be expected, particularly from the electron-phonon interaction.

II. PROCEDURES OF THE BAND CALCULATION

The wave function $\psi_n(\vec{k},\vec{r})$ of an electron belonging to band n and wave vector $\vec{k}$ is expanded as a linear combination of trial Bloch functions $\phi_j(\vec{k},\vec{r})$

$$\psi_n(\vec{k},\vec{r})=\sum_j c_{nj}(\vec{k})\,\phi_j(\vec{k},\vec{r})\ . \tag{1}$$

The $\phi_j(\vec{k},\vec{r})$ are linear combinations of Gaussian orbitals on the atomic sites,

$$\phi_j(\vec{k},\vec{r})=\frac{1}{\sqrt{N}}\sum_\mu e^{i\vec{k}\cdot\vec{R}_\mu}\,u_i(\vec{r}-\vec{R}_\mu)\ . \tag{2}$$

The orbitals u_i are products of normalized radial function of the form

TABLE I. Orbital exponents for the Gaussian basis set.

s type	p type	d type
10 000.0	100.0	2.50
800.0	11.0	0.36
90.0	2.5	0.14
16.0	0.7	
4.0	0.29	
1.4	0.15	
0.46		
0.24		
0.13		

$$R_{l_i}(r) = \left(\frac{2(2\zeta_i)^{l_i+3/2}}{\Gamma(l_i+\frac{3}{2})}\right)^{1/2} r^{l_i} e^{-\zeta_i r^2} \qquad (3)$$

(in which l_i is the relevant angular momentum and ζ_i is the orbital exponent) and angular functions which are real linear combinations of spherical harmonics. Our basis includes nine s-type, six p-type, and three d-type functions. The exponents are listed in Table I. The small exponents required in atomic calculations are not required to construct solid-state wave functions. The present basis can be compared to the nine s, seven p functions contracted to three independent s and three independent p functions employed in Ref. 17. Extensive tests in which the overlap matrix was diagonalized at many points in the Brillouin zone indicated that none of the overlap eigenvalues was small enough to cause numerical instability. The resulting Hamiltonian and overlap matrices are of dimension 42×42 at a general point of the Brillouin zone. The lattice constant was taken to be $6.597a_0$.[27]

The self-consistency calculation followed the procedures described in Refs. 22 and 25. Approximately twenty iterations were required to achieve self-consistency. The iterative process stopped when the (110) Fourier coefficient of the Coulomb potential did not change by more than 10^{-6} Ry. Changes in the lowest 100 rotationally independent Fourier coefficients of the crystal potential were considered. The charge density was sampled at 140 points in $\frac{1}{48}$ of the Brillouin zone in the final stages of the iterative process. The calculations were done using double precision arithmetic on an IBM 360-65.

The energy bands resulting from these calculations are shown along some directions of symmetry in Fig. 1. In order to facilitate comparison of our results with those of other workers, a table of energy levels relative to the lowest Γ_1 state is given in Table II. Results obtained by Dagens and Perrot[20] using the same exchange potential are also

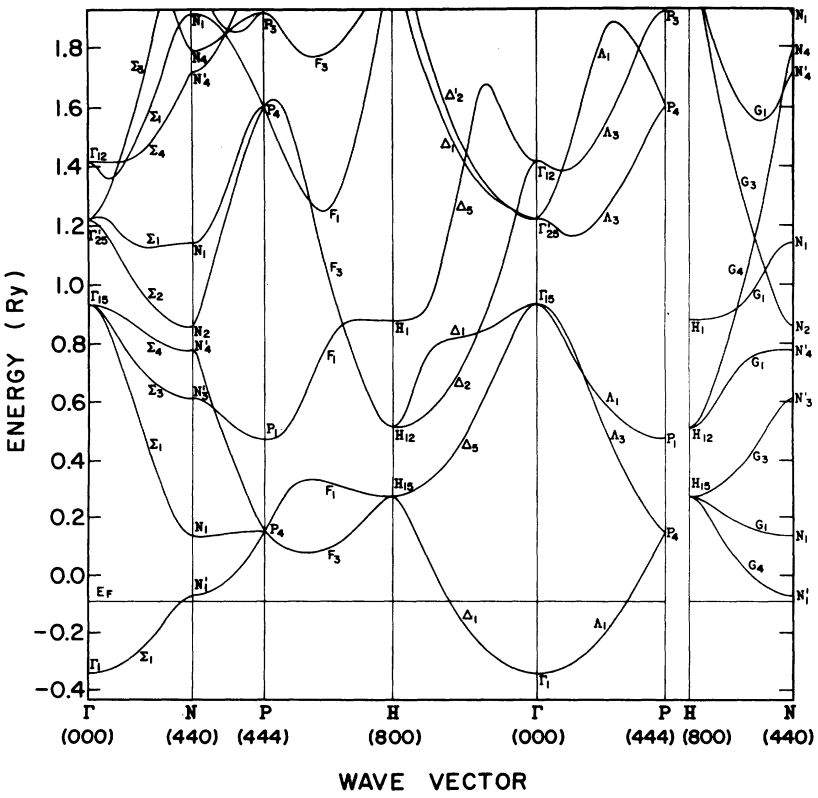

FIG. 1. Band structure of lithium in several symmetry directions.

TABLE II. Energies of selected states (in Ry). The results quoted from Ref. 20 pertain to the K-S exchange potential.

$2a\vec{k}/\pi$	State	$E(k)$ (present)	Ref. 20
(0,0,0)	Γ_1	0.000 00	0.000 00
(0,0,0)	Γ_{15}	1.274 04	1.275 54
(1,0,0)	Δ_1	0.042 10	0.042 15
(1,1,0)	Σ_1	0.083 82	0.083 85
(1,1,1)	Δ_1	0.125 99	0.126 00
(2,0,0)	Δ_1	0.170 74	0.171 22
(2,1,0)		0.208 39	0.208 53
(2,1,1)		0.250 66	0.250 63
(2,2,0)	N_1'	0.271 58	0.270 07
(2,2,0)	N_1	0.476 48	0.483 70
(2,2,0)	N_3'	0.954 96	0.982 12
(2,2,0)	N_4'	1.117 57	1.085 09
(2,2,2)	P_4	0.494 19	0.492 87
(2,2,2)	P_1	0.812 85	0.854 64
(4,0,0)	H_{15}	0.615 01	0.643 85
(4,0,0)	H_{12}	0.853 61	0.807 42
(4,0,0)	H_1	1.214 19	1.203 38

given. The calculation performed by these authors seems to differ from ours significantly only in that it was performed within the "muffin-tin approximation using the augmented-plane-wave (APW) method." There is evidently excellent agreement for states in the lowest band, but some of the excited states disagree by amounts up to 0.05 Ry. The origin of these discrepancies is not known, but may be related to the muffin-tin approximation.

III. FERMI SURFACE

The density of states was calculated from the energy levels according to Gilat-Raubenheimer method.[28] The Fermi energy was determined and the Fermi surface was constructed. The width of the occupied portion of the band ($E_F - E_{\Gamma_1}$) is 0.254 Ry. Our calculated Fermi surface is a slightly distorted sphere. The largest distortion is a bulge extending to about 4% of the average radius along the [110] axis. The surface does not touch the zone boundary. The distortions are conveniently characterized by parameters

$$\eta(\hat{k}) = 10^4 \, \frac{k_F(\hat{k}) - k_F^0}{k_F^0} \ , \tag{4}$$

in which $\hat{k}$ indicates a direction, $k_F(\hat{k})$ is the distance to the surface in that direction, and k_F^0 is the radius of the free-electron Fermi sphere. Our calculated values for η in the [100], [110], and [111] directions are given in Table III. The largest distortion from spherical shape is about 4% in the [110] direction. These results can be compared with the estimates of Donaghy and Stewart obtained from positron-annihilation experiments.[29] However, the interpretation of such experiments is not straightforward as there may be substantial corrections resulting from deviations of the electron and positron wave function from plane waves.[30] Recently, de Haas–van Alphen oscillations have been observed in a sample of lithium dispersed in paraffin wax.[31] These observations do not yield precise dimensions of the Fermi surface, but do show that the distortion from spherical form is small.

We have calculated the optical and thermal effective masses according to

$$\frac{m_{\rm op}}{m} = 6\left(\frac{2\pi}{a}\right)^3 \left(\int d^3k \, \nabla^2 E(\vec{k}) \right)^{-1} \tag{5}$$

and

$$\frac{m_{\rm th}}{m} = \frac{1}{2\pi k_F} \int \frac{dS_F}{|\nabla_k E(\vec{k})|} \ . \tag{6}$$

The integration of (5) was carried out using an empirical fit to $E(\vec{k})$ using a Kubic harmonic expansion through sixth order as in Ref. 10. Equation (6) was integrated numerically over the Fermi surface using an adaption of the linear analytic (Gilat-Raubenheimer) method used to compute the density of states. We find $m_{\rm op}/m = 1.48$ and $m_{\rm th}/m = 1.53$. These results agree well with values of 1.47 and 1.50 calculated by Perdew and Vosko.[21] Our results for these and other related parameters are summarized in Table IV, which also contains experimental and some other theoretical results. Comparison of the calculated and measured[32] thermal effective mass indicates a mass enhancement of 44%.

IV. OPTICAL CONDUCTIVITY

The real part of the frequency-dependent optical conductivity contains an interband contribution which is, for $\omega > 0$,

$$\begin{aligned} \mathrm{Re}[\sigma(\omega)] = \frac{2\pi e^2}{3m^2\omega} \sum_{ln} \int \frac{d^3k}{(2\pi)^3} \\ \times |\langle l\vec{k}|\vec{p}|n\vec{k}\rangle|^2 f_l(\vec{k})[1 - f_n(\vec{k})] \\ \times \delta(E_n(\vec{k}) - E_l(\vec{k}) - \hbar\omega) \ . \end{aligned} \tag{7}$$

In this equation, ω is the frequency of the light and $f_l(\vec{k})$ is the Fermi distribution function for the state $|l\vec{k}\rangle$ (wave vector $\vec{k}$, band l). The matrix elements involved in this formula were computed numerically using the wave functions obtained in the band calculation. Such a procedure is relatively easy to implement within the framework of the LCAO method of band calculation, since the matrix elements

TABLE III. Distortion of the Fermi surface in lithium. The parameter η is defined in Eq. (4).

	Present	Expt. (Ref. 28)
$\eta(100)$	−220	−100
$\eta(110)$	380	400
$\eta(111)$	−110	−100

TABLE IV. Parameters relating to the band structure and optical properties: m_{op} is the optical effective mass, m_{th} is the thermal mass; $G(E_F)$ is the density of states at the Fermi surface; ω_0 is the direct interband threshold; ω_p is the plasma frequency (computed with m_{op}); ω_L is the frequency at which the real part of the dielectric function vanishes; and κ_A is the effective ionic polarizability. Numbers in parentheses refer to the references.

Parameter	Present results	Other theoretical results	Experimental values
m_{op}/m	1.48	1.45 (12), 1.48 (21)	1.33 (34), 1.57 (36)
m_{th}/m	1.53	1.64 (12), 1.64 (20) 1.65 (16), 1.50 (21)	2.19 (32)
$G(E_F)$ (Ry^{-1})	6.54		
$E(\Gamma_1)$ (Ry)	−0.3454		
$E_F - E(\Gamma_1)$ (Ry)	0.2537	0.252 (12), 0.2601 (20)	
$E(N_1) - E(N_1')$ (Ry)	0.2048	0.209 (12), 0.214 (20) 0.210 (21)	
ω_0 (eV)	3.28	3.6 (12), 3.4 (21)	2.5 ± 0.1 (34), 3.2 (36)
ω_p (eV)	6.62		
ω_L (eV)	6.85		
κ_A	0.015		

of the gradient operator between Gaussian orbitals on different sites can be obtained analytically.[33] The wave-vector dependence of the matrix elements is significant. The integration over the Brillouin zone was performed by the Gilat-Raubenheimer method based on 1785 points in $\frac{1}{48}$ of the Brillouin zone. We have also computed the conductivity with the inclusion of a phenomenological constant relaxation time τ. In this case, the complex conductivity is

$$\sigma(\omega) = \frac{iNe^2}{m_{op}(\omega + i/\tau)} - \frac{2}{3}\frac{ie^2}{m^2\hbar}(\omega + i/\tau)\sum_{ln}\int \frac{d^3k}{(2\pi)^3}\frac{|\langle l\vec{k}|\vec{p}|n\vec{k}\rangle|^2}{\omega_{nl}}\frac{f_l(\vec{k})[1-f_n(\vec{k})]}{\omega_{nl}^2 - (\omega + i/\tau)^2} . \quad (8)$$

Here

$$\omega_{nl} = [E_n(\vec{k}) - E_l(\vec{k})]/\hbar ,$$

m_{op} is the optical effective mass given by (5), and N is the average electron density. It can be verified that this expression satisfies the sum rule

$$\int \mathrm{Re}[\sigma(\omega)]\,d\omega = \pi Ne^2/2m . \quad (9)$$

Our results for the real part of the conductivity are shown in Fig. 2 according to Eqs. (7) and (8). In the latter case, the relaxation time τ was chosen so that the Drude contribution, which comes from the first term of (8), fits the observed conductivity well below the interband threshold. We find $\tau = 9.86\times10^{-14}$ sec. The experimental results of Mathewson and Myers obtained from lithium films deposited on sapphire[34,35] are shown. Observations in a more limited energy range have been reported by Hodgson.[36]

The experimental observations do not extend to high enough energies to determine whether there is agreement with theory in regard to the general shape of the interband conductivity. The measurements do appear to indicate that the onset of interband transitions occurs at a lower energy than is predicted by our calculations. Some of the discrepancy is probably due to indirect (phonon-assisted) transitions. However, if such transitions are taken into account the onset of interband would

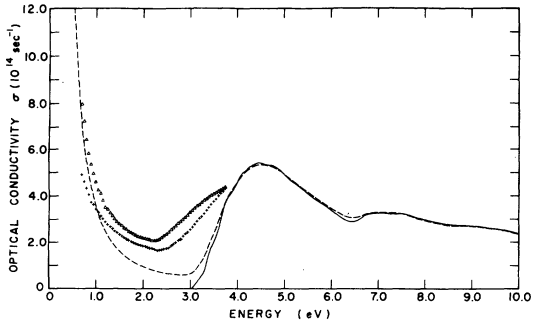

FIG. 2. Optical conductivity of lithium. The solid curve is obtained from Eq. (7), the dashed curve is obtained from Eq. (8) including a relaxation time $\tau = 9.68 \times 10^{-14}$ sec. The crosses and triangles are the result of Ref. 34 for temperatures of 140 and 298 °K, respectively.

TABLE V. Total energy of lithium. Quantities refer to Eq. (10). All energies are in rydbergs.

Sum of one electron energies	−6.970
$\frac{1}{2}$ Coulomb energy of electrons	8.577
$\frac{1}{3}$ exchange energy	−1.036
Total energy of solid	−14.511
Total energy of free atom	−14.387
Cohesive energy (calc.)	0.124
Cohesive energy (expt.) (Ref. 39)	0.122

be expected to be displaced from the calculated direct gap of 3.28 eV to perhaps ~3.00 eV $[E(N_1)-E_F$ minus phonon energy] which remains larger than the observed value (~2.4 eV at 125 °K). Our results for the gap at N are in good agreement with many other theoretical calculations, involving different potentials, and it is not likely that improved one-electron calculations can change this result substantially. It is possible that many-body effects may be involved. However, it is also possible that the measurements made on evaporated films are not representative of bulk single-crystal lithium. Our value for the onset of direct transitions agrees well with the result of Hodgson (3.2 eV) although the shape of the conductivity curve is different.[36] The recent calculation of Perdew and Vosko gives 3.4 eV for this quantity.[21]

One further comparison is of interest. The calculated optical conductivity of lithium differs qualitatively from that obtained in our previous work for potassium[26] in that the large absorption found in the 6–9-eV range in potassium was absent in lithium. This absorption was attributed to transitions involving d-like bands above the Fermi surface. In lithium, the corresponding bands are much higher in energy.

A quantity related to the low-energy (infrared) optical properties is the effective ionic polarizability.[37] This quantity, denoted κ_A, enters the expression for the real part of the dielectric function κ for photon energies much smaller than the threshold for interband transitions. If this condition is satisfied, and $\omega \gg 1/\tau$, where τ is the "Drude" relaxation time,

$$\kappa = 1 + \kappa_A - \omega_p^2/\omega^2 , \tag{10}$$

in which ω_p is the plasma frequency,

$$\omega_p^2 = 4\pi N e^2/m_{op}^* . \tag{11}$$

The polarizability κ_A is given by[38]

$$\kappa_A = \frac{8\pi e^2}{m^2\hbar} \sum_{nl} \int \frac{d^3k}{(2\pi)^3} f_l(\vec{k})[1-f_n(\vec{k})] \frac{|\langle l\vec{k}|\vec{p}|n\vec{k}\rangle|^2}{[\omega_{nl}(\vec{k})]^3} , \tag{12}$$

with

$$\omega_{nl}(\vec{k}) = \hbar^{-1}[E_n(\vec{k}) - E_l(\vec{k})] . \tag{13}$$

We have computed κ_A using the energies and matrix elements previously discussed. Our result is listed in Table IV. In addition, we have determined the frequency ω_L at which the real part of κ vanishes from our numerical calculation of σ [not from (10)]. This value, which corresponds closely to the peak of the energy-loss function, $\mathrm{Im}(1/\kappa)$, is found to be 6.85 eV.

V. COHESIVE ENERGY

Calculation of the cohesive energy furnishes a stringent test of the numerical accuracy of a band calculation, since this quantity is, if calculated directly, the difference of two much larger numbers. We have computed the total energy per atom of lithium metal using an expression for the total energy in the statistical-exchange approximation:

$$E_T = \frac{1}{N}\left(\sum_{n,\vec{k},\sigma} E_n(\vec{k}) - \frac{e^2}{2} \iint \frac{\rho(\vec{r})\rho(\vec{r}')\,d^3r\,d^3r'}{|\vec{r}-\vec{r}'|} - \frac{1}{4}\int \rho(\vec{r}) V_x(\vec{r})\,d^3r \right) , \tag{14}$$

in which $\rho(\vec{r})$ is the electron charge density, and $V_x(\vec{r})$ is the exchange potential

$$V_x(\vec{r}) = -2e^2(3\rho/8\pi)^{1/3} . \tag{15}$$

The summation in the first term includes occupied states only. The value obtained in this way for metallic lithium (at the observed lattice constant only) can be compared with similar results for the free lithium atom. Our results for the terms in Eq. (14) are presented in Table V. The uncertainty in the calculated solid-state total energy is believed to be ±0.01 Ry. The energy quoted for the free lithium atom was obtained in a separate calculation using same exchange potential ($\alpha = \frac{2}{3}$), but allowing for the spin polarization which exists in the atom. Our calculated free-atom energy is lower than that obtained if spin polarization is neglected by approximately 0.04 Ry.

The resulting cohesive energy is in excellent agreement with the experimental value given by Gschneider.[39] It also agrees quite well with that obtained by Averill with the same exchange approximation but using the APW method and a muffin-tin potential.[40] However, our calculated solid-state total energy is lower than that obtained by Averill by about 0.04 Ry, compensating for the lower total energy of the free atom. In addition, it has to be remembered that the $X\alpha$ approximation does not

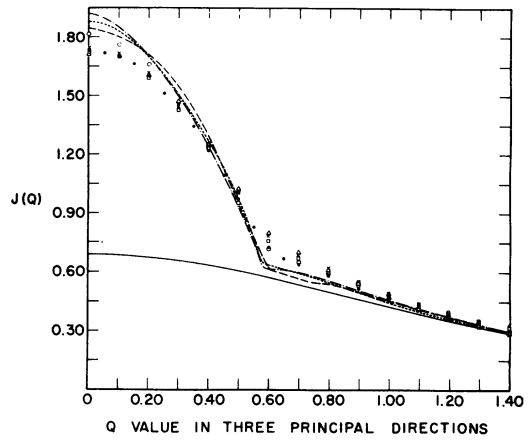

FIG. 3. Compton profile of lithium. The solid line is the core (1s) contribution. The other curves include the band electrons, and pertain to the following directions: dash-dot, [111] direction; short dashes, [100] direction; longer dashes, [110] direction. The experimental points are as follows: ×, Ref. 43, [111] direction; □, Ref. 43, [100] direction; Δ, Ref. 43, [110] direction; ○, Ref. (43), polycrystalline sample; and •, Ref. 42, polycrystalline sample.

take explicit account of electron correlation either in the atom or in the solid.

VI. COMPTON PROFILE

The Compton profile is a measure of the electron momentum distribution. Let $\vec{p}$ denote the initial momentum of an electron in the system, $\vec{k}$ denote the change in momentum after a Compton scattering event has occurred, and $\hbar\omega$ denote the energy transferred to the electron. In the impulse approximation it can be shown that the cross section for scattering into a fixed directon of k is proportional to[41]

$$J_{\hat{k}}(q) = \frac{\Omega}{(2\pi)^3} \int d^3p\, \rho(\vec{p})\, \delta(q - \vec{p}\cdot\hat{k}) \,, \tag{16}$$

in which $\rho(\vec{p})$ is the momentum distribution function Ω is the volume of the unit cell, $\hat{k} = \vec{k}/|\vec{k}|$, and

$$q = m\omega/|\vec{k}| - \tfrac{1}{2}|\vec{k}| \,. \tag{17}$$

A straightforward procedure exists for evaluation of $J_{\hat{k}}(q)$ using wave functions expressed as combinations of Gaussian orbitals. The details have been described previously.[42] Our results for $J_{\hat{k}}(q)$ are shown for three different directions in Fig. 3. Experimental results due to Phillips and Weiss[43] and Eisenberger *et al.*[44] are shown for comparison. It is apparent that the theoretical values of $J(q)$ are too large for small q and too small for large q. This discrepancy can reasonably be attributed to the effects of electron interactions, which tend to introduce additional high-momentum components into the wave function. The effects are, however, not large in lithium: Evidently most of the tail of the band contribution to $J(q)$ is accounted for in a one-electron band model. It should also be noted that our calculations reproduce the experimental directional anisotropy qualitatively but the magnitude of the anisotropy predicted is somewhat larger than is observed. Our results seem to be in good agreement with the APW calculation of Wakoh and Yamashita.[45]

*Supported in part by the U. S. Air Force Office of Scientific Research under Grant No. 71-2020.

[1]F. Seitz, Phys. Rev. 47, 400 (1935).
[2]J. Bardeen, J. Chem. Phys. 6, 367 (1938).
[3]R. H. Parmenter, Phys. Rev. 86, 552 (1952).
[4]R. A. Silverman, Phys. Rev. 85, 227 (1952).
[5]T. Wainwright and G. Parzen, Phys. Rev. 92, 1129 (1953).
[6]W. Kohn and N. Rostoker, Phys. Rev. 94, 1111 (1954).
[7]B. Schiff, Proc. Phys. Soc. Lond. A 67, 1 (1954).
[8]E. Brown and J. A. Krumnhansl, Phys. Rev. 109, 30 (1958).
[9]M. L. Glasser and J. Callaway, Phys. Rev. 109, 1541 (1958).
[10]J. Callaway, Phys. Rev. 124, 1824 (1961); Phys. Rev. 131, 2839 (1963).
[11]J. Callaway and W. Kohn, Phys. Rev. 124, 1824 (1962).
[12]F. S. Ham, Phys. Rev. 128, 82 (1962); Phys. Rev. 128, 2524 (1962).
[13]H. Schlosser and P. M. Marcus, Phys. Rev. 131, 2529 (1963).
[14]E. E. Lafon and C. C. Lin, Phys. Rev. 152, 579 (1966).
[15]P. M. O'Keefe and W. A. Goddard, III, Phys. Rev. Lett. 23, 300 (1969); Phys. Rev. 180, 747 (1969).
[16]W. E. Rudge, Phys. Rev. 181, 1033 (1969).
[17]R. C. Chaney, T. K. Tung, C. C. Lin, and E. E. Lafon, J. Chem. Phys. 52, 361 (1970).
[18]M. J. Lawrence, J. Phys. F 1, 836 (1971).
[19]S. T. Inoue, S. Anano, and J. Yamashita, J. Phys. Soc. Jap. 30, 1456 (1971).
[20]L. Dagens and F. Perrot, Phys. Rev. B 8, 1281 (1973).
[21]J. P. Perdew and S. H. Vosko, J. Phys. F (to be published).
[22]J. Callaway and C. S. Wang, Phys. Rev. B 7, 1096 (1973); R. A. Tawil and J. Callaway, Phys. Rev. B 7, 4242 (1973); J. Rath and J. Callaway, Phys. Rev. B 8, 5398 (1973).
[23]S. Huzinaga, J. Chem. Phys. 42, 1293 (1965).
[24]J. C. Slater, T. M. Wilson, and J. H. Wood, Phys. Rev. 179, 28 (1969).
[25]J. Callaway and J. L. Fry, in *Computational Methods in Band Theory*, edited by P. M. Marcus, J. F. Janak, and A. R. Williams (Plenum, New York, 1972), p. 512.
[26]W. Y. Ching and J. Callaway, Phys. Rev. Lett. 30, 441 (1973).
[27]C. S. Barrett, Acta Cryst. 9, 671 (1956).
[28]G. Gilat and L. J. Raubenheimer, Phys. Rev. 144, 390 (1966).
[29]J. J. Donaghy and A. T. Stewart, Phys. Rev. 164, 391 (1967).
[30]J. J. Paciga and D. L. Williams, Can. J. Phys. 49, 3227 (1971).
[31]D. L. Randles and M. Springford, J. Phys. F 3, L185 (1973).

[32]D. L. Martin, Proc. R. Soc. A 263, 378 (1961).
[33]Explicit expressions for these quantities are given by W. Y. Ching, Ph. D. thesis (Louisiana State University, 1974) (unpublished).
[34]A. G. Mathewson and H. P. Myers, Philos. Mag. 25, 853 (1972).
[35]A. G. Mathewson and H. P. Myers, Phys. Scr. 4, 291 (1971).
[36]J. N. Hodgson, in *Optical Properties and Electronic Structure of Metals and Alloys*, edited by F. Abeles (North-Holland, Amsterdam, 1966), p. 60.
[37]M. H. Cohen, Philos. Mag. 3, 762 (1958).
[38]J. Callaway, *Energy Band Theory* (Academic, New York, 1964), p. 298.
[39]K. A. Gschneider, Solid State Phys. 16, 275 (1964).
[40]F. W. Averill, Phys. Rev. B 6, 3637 (1972).
[41]P. M. Platzman and N. Tzoar, Phys. Rev. 139, A410 (1965).
[42]J. Rath, C. S. Wang, R. A. Tawil, and J. Callaway, Phys. Rev. B 8, 5139 (1973).
[43]W. C. Phillips and R. J. Weiss, Phys. Rev. B 5, 755 (1972).
[44]P. Eisenberger, L. Lam, P. M. Platzman, and P. Schmidt, Phys. Rev. B 6, 3671 (1972).
[45]S. Wakoh and J. Yamashita, J. Phys. Soc. Jap. 35, 1402 (1973).